Investigation of Physical Adhesion in Hemp Fibre Reinforced Composites Using Contact Angle Measurements and Inverse Gas Chromatography

Van de Vel, Sander; Saini, Gurleen Kaur ; Prapavesis, Alexandros ; Mosleh, Yasmine; Van Vuure, Aart Willem

Publication date
2025

Document Version
Final published version

Citation (APA)
Van de Vel, S., Saini, G. K., Prapavesis, A., Mosleh, Y., & Van Vuure, A. W. (2025). *Investigation of Physical Adhesion in Hemp Fibre Reinforced Composites Using Contact Angle Measurements and Inverse Gas Chromatography*. Paper presented at SAMPE EUROPE Conference 2025, Amsterdam, Netherlands.

INVESTIGATION OF PHYSICAL ADHESION IN HEMP FIBRE REINFORCED COMPOSITES USING CONTACT ANGLE MEASUREMENTS AND INVERSE GAS CHROMATOGRAPHY

Sander Van de Vel[1(*)], Gurleen Kaur Saini[1], Alexandros Prapavesis[1], Yasmine Mosleh[2], Aart Willem van Vuure[1]

[1]Department of Materials Engineering, KU Leuven, Leuven, Belgium
[2]Biobased Structures and Materials, Faculty of Civil Engineering and Geosciences, TU Delft, Delft, the Netherlands
(*) Email: sander.vandevel@kuleuven.be

1. ABSTRACT

This study investigates the interface between hemp fibre and thermoplastic polymer matrices such as polypropylene (PP) and poly-acrylate (Elium®). The analysis was conducted using both traditional dynamic contact angle measurements with various probe liquids and a more novel approach involving inverse gas chromatography (IGC) with multiple gaseous probes. The goal was to predict fibre–matrix compatibility based on surface chemical characterisation. Both methods showed good correlation, with the dispersive surface energy of the natural fibres ranging between 33 and 39 mJ/m², and a significant basic component contributing to the overall polar surface energy. IGC proved more effective at distinguishing between the predominantly apolar PP and the more polar poly(methyl methacrylate) (PMMA) based Elium, with the predicted thermodynamic work of adhesion notably higher for hemp–Elium interfaces compared to hemp–PP. Micromechanical testing, combined with microscopic imaging, further supported the observation of improved intermolecular adhesion between the natural fibres and the Elium matrix.

2. INTRODUCTION

2.1 Natural Fibre Composites

Natural fibres have attracted increasing attention for their potential use in composite materials, owing to their favourable specific properties and lower environmental impact compared to traditional reinforcements such as glass fibres. Fibres like flax and hemp offer high specific strength and stiffness, making them promising candidates for advanced composite applications [1]. Their cultivation and extraction require significantly less energy than the production of glass or carbon fibres, further enhancing their appeal as environmentally sustainable alternatives [2].

However, as emphasized by Wambua et al. [1], the key challenge in developing high-performance natural fibre composites lies in achieving effective fibre–matrix adhesion. The interfacial region plays a critical role in stress transfer, and insufficient adhesion can severely limit composite performance. Natural fibres are typically hydrophilic, while most thermoplastic matrices are hydrophobic, resulting in poor interfacial compatibility. A thorough understanding of the physicochemical interactions at the fibre–matrix interface is therefore essential, particularly for high-end applications where maximizing reinforcement efficiency is crucial.

3. MATERIALS AND METHODS

3.1 Flax and Hemp Fibres

All hemp fibres used were grown in France and extracted via either scutching/hackling or by breaking rollers/cards [3]. One batch—hemp fibre (1)—was of the Fedora variety and was extracted using the breaking card method by HempAct in 2011. A second batch—hemp fibre (2)—was a 2024 mixed-variety batch processed by EcoTechnilin from hackled hemp. As a benchmark, flax fibres were also included since flax is more widely used in (semi-)structural applications. Flax fibres were sourced as FLAXTAPE® 200 (2024) from EcoTechnilin (France). Fibre surfaces were not washed or smoothed prior to analysis to retain as much as possible their actual surface energy profiles as used in composite applications.

3.2 Thermoplastic Polymers

Elium® 151XO/191SA (Arkema, France), a methyl methacrylate (MMA)-based monomer blend, was selected for its low viscosity and suitability for infusion. Polymerization of the monomers was initiated by adding Butanox M50 (ketone peroxide, Nouryon, Netherlands) with a ratio of 1.5/100 peroxide to monomer. Elium films were produced via film casting which were used directly for contact angle measurements or grinded into a powder for IGC measurements. Polypropylene was obtained as homopolymer granules from Goodfellow and processed into thin films via thermocompression using a Fontijne Grotnes LabEcon TP400 press. These films were used for contact angle measurements and cut into fine fibres for IGC.

3.3 Contact Angle Measurements

Contact angle (CA) measurements were performed with the tensiometer Krüss K100 using a contact line velocity of 1.5mm/min with four analytical grade probe liquids (ultrapure water: 18,2 Ω cm resistivity, Ethylene Glycol, 1-Bromonaphthalene and Bromoform). The CA between the advancing and receding liquid front on a fibre or polymer film was determined using the Wilhelmy plate method adapted for single fibre test filaments as described by Fuentes et al. [4], and is based on the molecular-kinetic wetting theory by Blake [5].

When a plate or fibre is immersed in or withdrawn from a liquid, a sensitive microbalance within a tensiometer can measure the total force acting on the solid material (F_{total}). This force is the result of the capillary rise of the probe liquid on the solid surface ($F_{capillary}$), the gravitational force acting on the solid ($F_{gravitational}$) and the buoyancy force due to the displacement of the probe liquid by the solid ($F_{bouyancy}$) Eq. (1).

$$F_{total} = F_{capillary} + F_{gravitational} - F_{bouyancy} \quad (1)$$

By zeroing the balance at the start of the measurement, before contact with the probe liquid, the gravitational component of the force can be neglected as long as the absorption of probe liquid by the solid remains negligible during the measurement. The buoyance force can either be neglected for fibres, as this will be several orders of magnitude below the capillary force, or calculated and subtracted for plates with precisely known dimensions. This leads to the following equation where the measured force ($F_{measured}$) can be related to the dynamic contact angle of the capillary between the liquid and the solid (θ), the perimeter of a fibre or plate (p) and the surface tension of the probe liquid (γ_l) Eq. (2).

$$F_{measured} = p\,\gamma_l \cos\theta \tag{2}$$

For polymer films or plates, the perimeter was measured using a Mitutoyo calliper with a precession of ±10 µm. However, this is not feasible for irregular surfaces, particularly those of natural fibres. To overcome this, a probe liquid with very low surface tension—such as hexane (γ_l = 18.4 mJ/m²)—was used. At low advancing speeds, such liquids yield a CA close to zero, allowing the local perimeter of irregular objects to be accurately determined and subsequently used in Eq. (2).

After measuring both the advancing and receding contact angles, the equilibrium contact angle can be calculated using Eq. (3). The equilibrium contact angle is the most reliable approach for further surface energy calculations, as it is the only value which provides a full overview of all surface interactions [6].

$$\cos\theta_{equ} = \frac{\cos\theta_{adv} + \cos\theta_{rec}}{2} \tag{3}$$

3.4 Surface Energy and Interfacial Parameters

The surface energy components of a solid can be calculated from contact angle measurements using the Van Oss, Chaudhury and Good model (vOCG) [7]. They considered the intermolecular interaction to be made up of a dispersive or Lifshitz–van der Waals component (γ^{LW}) and a polar component, which is further split into an electron-acceptor (acid, γ^+) and an electron-donor (basic, γ^-) component. The relationship between energy components of a solid, energy components of a liquid and the equilibrium angles between the solid and liquid is given by Eq. (4).

$$A\,x = b \tag{4}$$

Where, $A = \begin{bmatrix} \sqrt{\gamma_{l,1}^{LW}} & \sqrt{\gamma_{l,1}^{+}} & \sqrt{\gamma_{l,1}^{-}} \\ \sqrt{\gamma_{l,2}^{LW}} & \sqrt{\gamma_{l,2}^{+}} & \sqrt{\gamma_{l,2}^{-}} \\ \sqrt{\gamma_{l,3}^{LW}} & \sqrt{\gamma_{l,3}^{+}} & \sqrt{\gamma_{l,3}^{-}} \end{bmatrix}$; $x = \begin{bmatrix} \sqrt{\gamma_s^{LW}} \\ \sqrt{\gamma_s^{+}} \\ \sqrt{\gamma_s^{-}} \end{bmatrix}$; $b = \begin{bmatrix} \gamma_{l,1}(1+\cos\theta_1)/2 \\ \gamma_{l,2}(1+\cos\theta_2)/2 \\ \gamma_{l,3}(1+\cos\theta_3)/2 \end{bmatrix}$

Once the surface energy components of two materials are known, the interfacial energy (γ_{sl}) between them can be calculated with Eq. (5). This interfacial energy value reflects the strength of adhesion between two materials, with lower values indicating stronger adhesion. For optimal adhesion, γ_{sl} should be minimized [8].

$$\gamma_{sl} = \gamma_s^{LW} + \gamma_l^{LW} + 2\left[\sqrt{\gamma_s^{+}\gamma_s^{-}} + \sqrt{\gamma_l^{+}\gamma_l^{-}} - \sqrt{\gamma_s^{LW}\gamma_l^{LW}} - \sqrt{\gamma_s^{+}\gamma_l^{-}} - \sqrt{\gamma_s^{-}\gamma_l^{+}}\right] \tag{5}$$

From the interfacial energy and the total surface energy of both the fibre reinforcement (γ_s) and polymer matrix (γ_l), the thermodynamic work of adhesion (W_a) can be calculated with Eq. (6) [9]. This value represents the work needed to overcome intermolecular interactions and to

separate two surfaces. In literature, work of adhesion has often been correlated with the strength of an interface [10], [11], [12], [13], [14].

$$W_a = \gamma_s + \gamma_l - \gamma_{sl} \tag{6}$$

Raw data collected from the Krüss K100 tensiometer was processed using MATLAB code to determine advancing and receding contact angles. Surface energy values for all investigated solids were determined using *SurfTen* 4.3 software, developed by Claudio Della Volpe.

3.5 Mechanical Testing

For assessing the mechanical performance of the fibre-matrix interface, transverse three-point bending (T3PB) can be applied following ASTM D7264/D7264M-07. Composite plates were produced using fibres of the Fedora 2011 variety—hemp fibre (1)—and either thermocompression for the PP matrix ($V_f = 54\%$) or vacuum-assisted resin infusion for Elium ($V_f = 26\%$) and epoxy ($V_f = 37\%$). The epoxy (Epikote 828 LVEL with 1,2-diaminocyclohexane (Dytek DCH-99) hardener) was added as reference.

All bending tests were performed using an Instron 5943 equipped with a 1kN load cell and a three-point bending setup with 64mm span and a 2mm/min crosshead displacement. The transverse bending stiffness ($E_{C-Transverse}$) was normalized to a fibre volume fraction of 40% using Chamis's equation, Eq. (7) [15].

$$E_{C-Transverse} = \frac{E_m}{1 - \sqrt{V_f} * (1 - \frac{E_m}{E_{f-transverse}})} \tag{7}$$

Scanning electron microscopy (SEM) was further used to investigate the fracture surface and to identify the type of failure that occurred.

3.6 Inverse Gas Chromatography

Another technique that can be used to determine dispersive and acid–base surface interactions is inverse gas chromatography, which employs various probe gases. When using IGC at infinite dilution, the injected probe quantity is so low that probe–probe interaction can be neglected [16]. The probe gases are injected along with a non-reacting carrier gas, typically helium, and the eluting probe molecules are measured using a flame ionization detector. The retention time of each injected probe is recorded, and it directly correlates with the net retention volume V_N, taking into account the flow at the exit of the column and the James–Martin correction factor for gas compressibility [17]. The retention volume is related to the free energy change of adsorption ($\Delta G_{ads-probe}$) by Eq. (8), where R is the universal gas constant and T is the measurement temperature [18], [19].

$$\Delta G_{ads-probe} = -R\,T\,\ln(V_N) \tag{8}$$

Since *n*-alkanes possess only a dispersive component in their surface energy, Dorris and Gray demonstrated that the dispersive component of a solid surface can be determined by injecting a series of *n*-alkanes and analysing the incremental free energy change associated with the addition of a single methylene group to the alkane probe ($\Delta G_{ads}^{CH_2}$). This results in Eq. (9) where

γ_s^d is the dispersive energy component of the solid, γ_{CH_2} is the energy of a solid made only of methylene units and a_{CH_2} is the cross-sectional area of a methylene group [18], [19].

$$\gamma_s^d = \frac{1}{\gamma_{CH_2}} \left[\frac{\Delta G_{ads}^{CH_2}}{2\, N_A\, a_{CH_2}} \right]^2 \tag{9}$$

Using polar probes also enables the determination of the polar character of a surface through the acidity (K_a) and basicity (K_b) constants of the solid. The free energy change of adsorption for each polar probe can be compared to the linear *n*-alkane reference line by applying a topological index that accounts for molecular geometry and relates each polar probe to the non-polar alkanes [20]. The deviation between the adsorption energy of a polar probe and the alkane reference line reflects specific (polar) interactions with the solid surface. These deviations allow for the calculation of the solid's acidity and basicity constants, based on the electron donor (DN) and acceptor (AN) values of each probe as defined by the semi-empirical scale of Gutman [21] Eq. (10).

$$I_{SP} = \Delta G_{ads}^{SP} = DN\, K_a + AN\, K_b \tag{10}$$

Measurements were performed using an adapted gas chromatography apparatus from Thermo Fisher Scientific (Trace 1310 Gas Chromatograph), with data analysis conducted using software from Adscientis, France (Nucleus v.3.3.7, SolID v.3.3.4). The columns used for natural fibres were 100 cm in length with an internal diameter of 4.57 mm and were filled with 5 to 6 grams of long technical fibres. The columns for Elium were 60 cm in length and filled with 6 grams of powdered Elium. For PP, the columns measured 80 cm in length and were filled with 6 grams of short PP fibres.

4. RESULTS

4.1 Contact angle measurements

When selecting test liquids for contact angle measurements, it is advisable to choose a set of three liquids that span a broad range of surface interactions with the solid. Commonly, water is used for its relatively high acidic surface energy, ethylene glycol for its basic character, and 1-bromonaphthalene as a liquid exhibiting purely dispersive interactions. However, due to the typically hydrophilic nature of natural fibres, accurately measuring the receding contact angle with water becomes challenging. Water can easily be entrapped mechanically around surface roughness, which leads to an over-estimated capillary weight. Receding contact angles are generally lower than advancing angles, and the strong interaction with water often causes the receding angle to approach zero for natural fibres. This is illustrated in Figure 1, where the receding angle with water could not be determined for a hemp fibre.

As an alternative, bromoform was proposed to replace water, as it also probes primarily acidic interactions but has a lower overall surface energy, thus reducing the intensity of interactions with the fibre surface. Figure 1 demonstrates the feasibility of using bromoform for natural fibres, as both advancing and receding angles could be successfully measured. However, when used on polymer films, bromoform proved unsuitable due to its tendency to cause unpredicted polymer interactions. These interactions increased the measured contact angle over time, as shown in Figure 1.

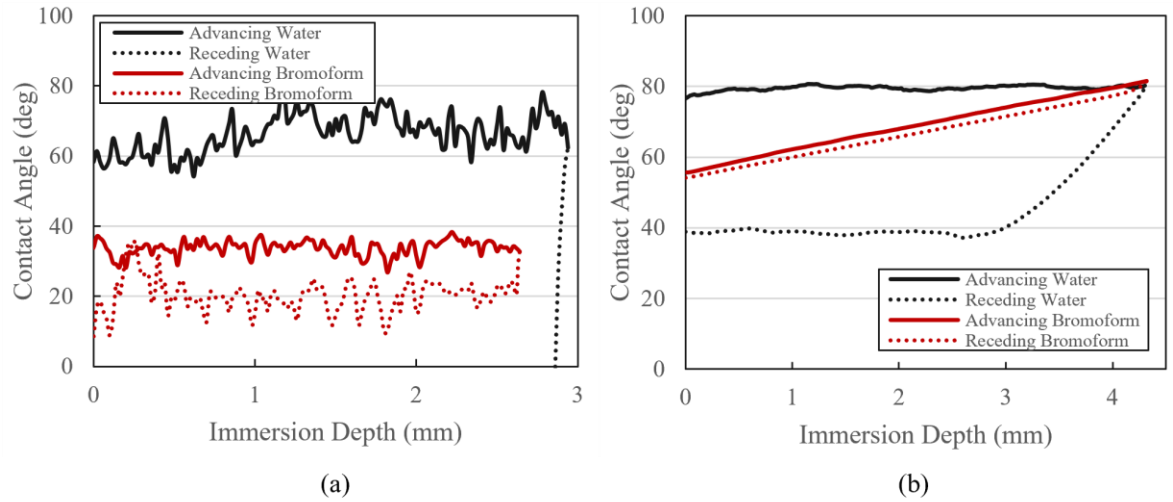

Figure 1. Graphs displaying the different interaction of water and bromoform with natural fibres (a) and polymer films (b).

Since bromoform was not suitable for measurements on polymer films, water was used for further analysis. For calculating the equilibrium contact angles, the receding contact angles with water were assumed to be zero for hemp fibre (1) and hemp fibre (2). The results of all contact angle measurements are summarized in Table 1. As indicated by the advancing contact angle with water exceeding 90°, the FlaxTape 200 from EcoTechnilin exhibits greater hydrophobicity than the hemp fibres investigated in this study. This increased hydrophobicity also reduced the interaction with water, enabling the measurement of receding contact angles using water. Both thermoplastic polymers also exhibit a more hydrophobic character than the hemp fibres, given by their advancing contact angles with water above 80°.

Table 1. Advancing, Receding and Equilibrium contact angles between natural fibres and polymer films with water (WT), ethylene glycol (EG) and bromonaphthalene (BrN) as test liquids.

	Hemp fibre (1)	Hemp fibre (2)	Flax fibre	Elium	PP
WT					
Adv	70.8 ± 4.7	60.9 ± 4.9	92.0 ± 6.9	86.2 ± 2.2	81.0 ± 1.3
Rec	-	-	55.7 ± 11.5	44.2 ± 7.1	60.0 ± 3.2
Equ	48.4 ± 3.0	42.0 ± 3.2	74.7 ± 8.5	67.0 ± 3.8	70.8 ± 2.1
EG					
Adv	61.1 ± 8.5	56.0 ± 6.3	68.4 ± 3.0	72.2 ± 2.0	78.8 ± 3.6
Rec	12.2 ± 1.6	13.7 ± 7.9	45.8 ± 8.7	51.5 ± 3.0	52.9 ± 4.5
Equ	43.1 ± 5.7	40.1 ± 5.5	57.8 ± 5.4	62.3 ± 2.4	66.5 ± 3.9
BrN					
Adv	40.4 ± 5.2	44.8 ± 4.0	56.2 ± 2.9	56.8 ± 4.8	77.3 ± 3.8
Rec	22.1 ± 1.6	31.8 ± 3.1	30.1 ± 2.7	52.7 ± 4.8	53.7 ± 1.9
Equ	32.4 ± 3.7	38.8 ± 3.5	44.7 ± 2.7	54.8 ± 4.8	66.1 ± 2.9

Based on the measured contact angles for both hemp fibre sources, flax fibres, Elium, and PP, the thermodynamic work of adhesion was calculated following the vOCG model to evaluate the adhesion potential of each fibre–matrix combination. Literature values for the surface energy components of polyvinylidene fluoride (PVDF) and polyoxymethylene (POM)—a copolymer of formaldehyde (CH_2O) and ethylene oxide (C_2H_4O)—were included as references for thermoplastic polymers known to exhibit good adhesion [14], [22]. Figure 2 presents the calculated W_a values for the three different fibre sources with each of the four matrices.

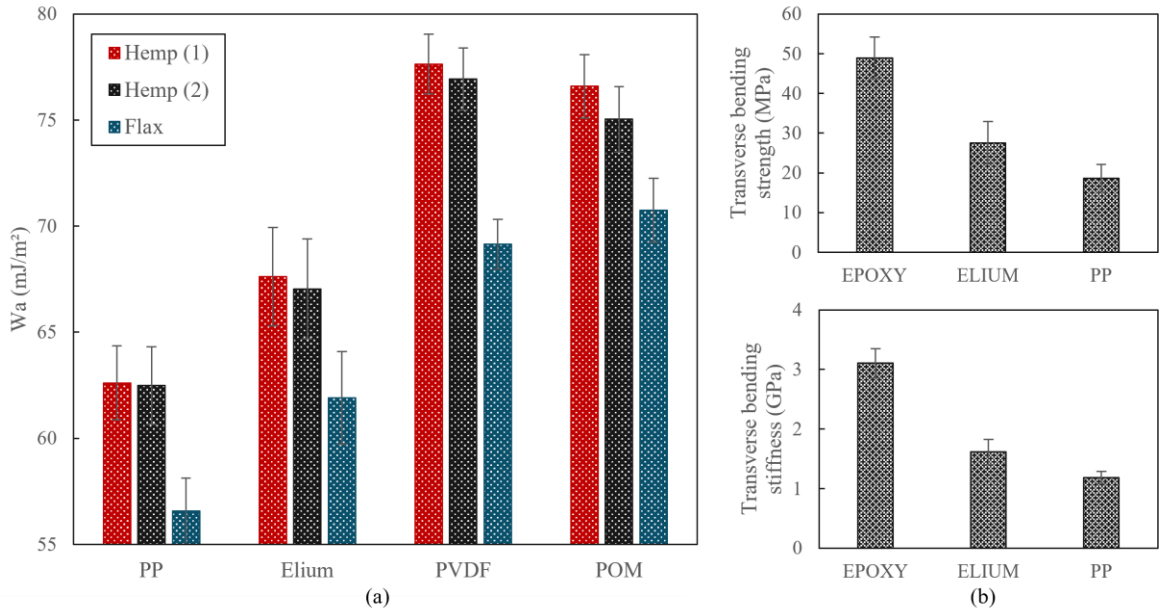

Figure 2. (a) Work of Adhesion between natural fibres and polymer matrices tested in this study; PP and Elium; or as found in literature; PVDF and POM [14], [22]. (b) Transverse bending properties for hemp fibre (1) composites.

As shown in Figure 2, polypropylene exhibits the lowest work of adhesion values across all fibre types. This is consistent with the chemical nature of PP, which can only form weak Van der Waals interactions—mainly London dispersion forces and limited interactions with polar sites on the fibre surface. In contrast, Elium, PVDF, and POM are polar polymers and can engage in stronger dipole–dipole interactions with the natural fibres, enhancing interfacial adhesion. The relatively long ester side chains of Elium may introduce steric hindrance during contact angle measurements, potentially leading to an underestimation of its actual work of adhesion compared to PVDF and POM.

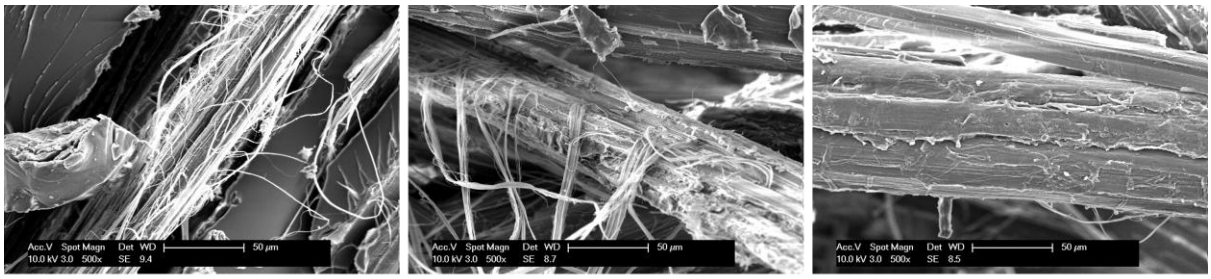

Figure 3. SEM images sowing the fracture surface after transverse three point bending for: (a) epoxy, (b) Elium, (c) PP.

To further assess the interfacial strength, mechanical tests were performed on composites made from hemp fibre (1) combined with epoxy, PP and Elium. Transverse bending tests were conducted, with a standard epoxy matrix included as a reference for ideal adhesion, given its ability to form covalent bonds with the fibre surface, and the results are summarized in Figure 2. The transverse bending strengths for epoxy, Elium, and PP were measured to be 49.0 ± 5.2 MPa, 27.6 ± 5.4 MPa, and 18.6 ± 3.5 MPa, respectively. The normalized bending stiffness follows the same trend with epoxy clearly outperforming both thermoplastic matrices, and Elium performing better than PP. Figure 3 also includes SEM images of the fracture sites after transverse bending tests. These results support the conclusion that Elium forms a stronger interface with the hemp fibres than PP, likely due to enhanced polar interactions and possible hydrogen bonding with hydroxyl groups on the fibre surface [23]. The SEM images show a

smooth fibre surface with PP and fractured fibre surfaces for Elium and epoxy, with exposed microfibrils. The covalent bonds between epoxy and natural fibres are still superior to the interaction with the thermoplastic matrices, resulting in the highest transverse bending strength.

Inverse gas chromatography was performed on the same materials as an alternative to contact angle measurements. The primary advantage of IGC is that it characterizes bulk surface properties using several grams of fibres or polymer powder, compared to contact angle techniques that often rely on single fibres or thin films. IGC also allows for a wider variety of probe molecules—including linear, branched, and cyclic alkanes, as well as a range of polar probes—thereby broadening its applicability.

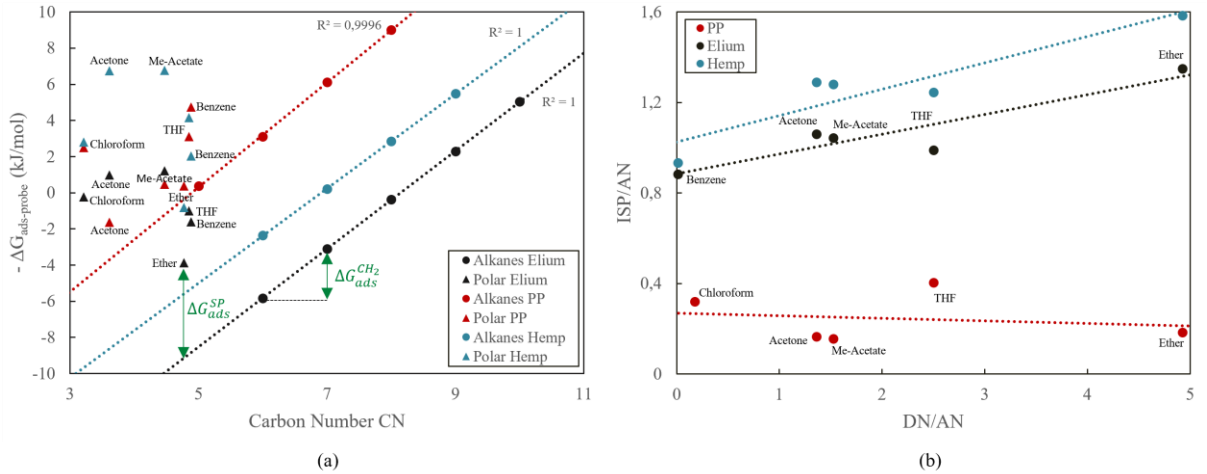

Figure 4. IGC results: (a) Measurements for the free energy of adsorption of n-alkane and polar probe molecules on hemp fibres, PP and Elium. (b) Determination of acidity and basicity constants using Gutmann's theory and based on measurements with several polar probe gases on hemp, PP and Elium.

For this study, only linear alkanes and certain polar probes were used and the results for hemp fibre (2), PP and Elium are depicted in Figure 4. It is found that for the dispersive component of the surface free energy (γ_s^d), both IGC and tensiometer data show good correlation for the natural fibres. From tensiometer measurements, the dispersive energy component for hemp fibre (1), hemp fibre (2) and flax were 39.7 ± 2.6 mJ/m², 39.4 ± 2.7 mJ/m² and 33.3 ± 2.0 mJ/m², respectively. Both IGC and tensiometer data also indicated that the natural fibres exhibited a predominantly basic surface character. Figure 4 (b) shows the calculation of the acidity and basicity constants using Gutmann's theory and indicates a satisfactory linear relation. The basic surface energy values obtained from contact angle measurements were 16.5 ± 2.0 mJ/m², 20.5 ± 2.2 mJ/m², and 5.4 ± 3.8 mJ/m² for hemp fibre (1), hemp fibre (2), and flax, respectively, while the acidic components were negligible (below 0 mJ/m²), consistent with the presence of free hydroxyl groups on the fibre surfaces. IGC further supports this with ratios of $\frac{K_a}{K_b} < 0.9$ for all natural fibres, indicating a predominantly basic surface [24].

For the polymers, IGC measured a higher dispersive component compared to the natural fibres. In contrast, contact angle measurements yielded lower dispersive values for both PP and Elium, with values of 21.9 ± 1.5 mJ/m² and 27.6 ± 2.4 mJ/m², respectively. These values appear relatively low for polymers, especially considering literature values such as 38.5 ± 0.5 mJ/m² for PMMA [25] and 29.9 ± 0.5 mJ/m² for PP [10]. For Elium, both IGC and contact angle measurements provided consistent results, including a basic surface energy of 11.0 ± 2.4 mJ/m². However, the contact angle method appeared to overestimate the basicity of PP (10.9 ±

1.5 mJ/m²), which is unexpected given that pure PP typically only exhibits weak dispersive interactions. IGC proved more effective in revealing the limited acidic/basic interactions of PP compared to the other tested materials, as seen in Figure 4 (b) and indicated by the lower K_a and K_b values.

Table 2. Dispersive energy as determined by IGC measurements and the acidity (K_a) and basicity (K_b) constants.

	Hemp fibre (1)	Hemp fibre (2)	Flax fibre	Elium	PP
γ_s^d (mJ/m²)	38.9 ± 0.3	37.1 ± 0.3	36.4 ± 0.6	40.2 ± 0.2	45.7 ± 1.3
K_a	0.117	0.049	0.061	0.087	-0.012
K_b	1.026	1.053	0.963	0.886	0.270
K_a/K_b	0.114	0.047	0.063	0.098	-0.044

Since the PP used in this study was delivered in granule form, thin films had to be processed in-house to enable contact angle measurements. This processing step may have introduced foreign molecules or additives into the PP sheets, potentially explaining the unexpected presence of a basic surface energy component. Additionally, contact angle measurements are more sensitive to factors such as surface roughness and are conducted on a much smaller sample size compared to IGC. These limitations may contribute to variability in the contact angle data, making the IGC results appear generally more reliable for assessing surface energy characteristics.

5. CONCLUSIONS

This study demonstrates that hemp fibres exhibit a more hydrophilic surface character than commercial flax fibres, as indicated by lower advancing water CA's and the inability to measure receding angles with water. Among the polymer matrices investigated, Elium showed better interfacial adhesion with hemp fibres than PP, supported by higher thermodynamic work of adhesion and transverse bending strength, as well as SEM observations of improved fibre-matrix interaction. However, compared to polymers such as PVDF and POM the compatibility is lower, indicating that improvement by fibre treatment development is necessary. Inverse gas chromatography provided surface energy results that correlated well with contact angle measurements, particularly for the dispersive and polar character of the natural fibres. Given its larger sample size and reduced sensitivity to surface roughness, IGC appears to be a more robust method for surface energy characterisation in these materials.

6. ACKNOWLEDGMENTS

This project has received funding from the Circular Bio-based Europe Joint Undertaking (CBE-JU) under grant agreement No101157517. The JU receives support from the European Union Horizon Europe research and innovation program and the Bio Based Industries Consortium.

7. REFERENCES

[1] P. Wambua, J. Ivens, and I. Verpoest, "Natural fibres: can they replace glass in fibre reinforced plastics?," *Compos Sci Technol*, vol. 63, no. 9, pp. 1259–1264, Jul. 2003, doi: 10.1016/S0266-3538(03)00096-4.

[2] Y. S. Song, J. R. Youn, and T. G. Gutowski, "Life cycle energy analysis of fiber-reinforced composites," *Compos Part A Appl Sci Manuf*, vol. 40, no. 8, pp. 1257–1265, Aug. 2009, doi: 10.1016/J.COMPOSITESA.2009.05.020.

[3] M. Grégoire *et al.*, "Analysis of the potential of hemp fibres for load bearing composite reinforcement using classical field management techniques and carded route," *Compos Part A Appl Sci Manuf*, vol. 190, p. 108658, Mar. 2025, doi: 10.1016/J.COMPOSITESA.2024.108658.

[4] C. A. Fuentes *et al.*, "Wetting behaviour and surface properties of technical bamboo fibres," *Colloids Surf A Physicochem Eng Asp*, vol. 380, no. 1–3, pp. 89–99, May 2011, doi: 10.1016/J.COLSURFA.2011.02.032.

[5] T. D. Blake, "The physics of moving wetting lines," *J Colloid Interface Sci*, vol. 299, no. 1, pp. 1–13, Jul. 2006, doi: 10.1016/J.JCIS.2006.03.051.

[6] C. A. Fuentes, *INTERFACIAL ADHESION IN NATURAL AND SYNTHETIC FIBRE COMPOSITES: A PHYSICAL-CHEMICAL-MECHANICAL APPROACH*, Dissertation. 2014.

[7] C. J. Van Oss, R. J. Good, and M. K. Chaudhury, "The role of van der Waals forces and hydrogen bonds in 'hydrophobic interactions' between biopolymers and low energy surfaces," *J Colloid Interface Sci*, vol. 111, no. 2, pp. 378–390, Jun. 1986, doi: 10.1016/0021-9797(86)90041-X.

[8] K. L. Mittal, "The role of the interface in adhesion phenomena," *Polym Eng Sci*, vol. 17, no. 7, pp. 467–473, Jul. 1977, doi: 10.1002/PEN.760170709;PAGEGROUP:STRING:PUBLICATION.

[9] J. C. Berg, "The importance of acid-base interactions in wetting, coating, adhesion and related phenomena," *Nord Pulp Paper Res J*, vol. 8, no. 1, pp. 75–85, Jan. 1993, doi: 10.3183/NPPRJ-1993-08-01-P075-085.

[10] C. A. Fuentes *et al.*, "Effect of physical adhesion on mechanical behaviour of bamboo fibre reinforced thermoplastic composites," *Colloids Surf A Physicochem Eng Asp*, vol. 418, pp. 7–15, Feb. 2013, doi: 10.1016/J.COLSURFA.2012.11.018.

[11] E. Pisanova, S. Zhandarov, and E. Mäder, "How can adhesion be determined from micromechanical tests?," *Compos Part A Appl Sci Manuf*, vol. 32, no. 3–4, pp. 425–434, Mar. 2001, doi: 10.1016/S1359-835X(00)00055-5.

[12] M. Nardin and J. Schultz, "Relationship between work of adhesion and equilibrium interatomic distance at the interface," *Langmuir*, vol. 12, no. 17, pp. 4238–4242, Aug. 1996, doi: 10.1021/LA9602168/ASSET/IMAGES/MEDIUM/LA9602168E00019.GIF.

[13] D. E. Packham, "Work of adhesion: contact angles and contact mechanics," *Int J Adhes Adhes*, vol. 16, no. 2, pp. 121–128, May 1996, doi: 10.1016/0143-7496(95)00034-8.

[14] W. Woigk *et al.*, "Interface properties and their effect on the mechanical performance of flax fibre thermoplastic composites," *Compos Part A Appl Sci Manuf*, vol. 122, pp. 8–17, Jul. 2019, doi: 10.1016/j.compositesa.2019.04.015.

[15] C. C. Chamis, "MECHANICS OF COMPOSITE MATERIALS: PAST, PRESENT, AND FUTURE," Oct. 1984.

[16] J. C. Berg, "Semi-empirical strategies for predicting adhesion," *Adhesion Science and Engineering*, pp. 1–73, Jan. 2002, doi: 10.1016/B978-044451140-9/50001-9.

[17] A. Van Asten, N. Van Veenendaal, and S. Koster, “Surface characterization of industrial fibers with inverse gas chromatography,” *J Chromatogr A*, vol. 888, no. 1–2, pp. 175–196, Aug. 2000, doi: 10.1016/S0021-9673(00)00487-8.
[18] G. M. Dorris and D. G. Gray, “Adsorption of n-alkanes at zero surface coverage on cellulose paper and wood fibers,” *J Colloid Interface Sci*, vol. 77, no. 2, pp. 353–362, Oct. 1980, doi: 10.1016/0021-9797(80)90304-5.
[19] G. M. Dorris and D. G. Gray, “Adsorption, spreading pressure, and london force interactions of hydrocarbons on cellulose and wood fiber surfaces,” *J Colloid Interface Sci*, vol. 71, no. 1, pp. 93–106, Aug. 1979, doi: 10.1016/0021-9797(79)90224-8.
[20] E. Brendlé and E. Papirer, “A New Topological Index for Molecular Probes Used in Inverse Gas Chromatography for the Surface Nanorugosity Evaluation,” *J Colloid Interface Sci*, vol. 194, no. 1, pp. 207–216, Oct. 1997, doi: 10.1006/JCIS.1997.5104.
[21] “The Donor-Acceptor Approach to Molecular Interactions | SpringerLink.” Accessed: May 11, 2025. [Online]. Available: https://link.springer.com/book/9781461588276
[22] L. Q. N. Tran, C. A. Fuentes, C. Dupont-Gillain, A. W. Van Vuure, and I. Verpoest, “Understanding the interfacial compatibility and adhesion of natural coir fibre thermoplastic composites,” *Compos Sci Technol*, vol. 80, pp. 23–30, May 2013, doi: 10.1016/j.compscitech.2013.03.004.
[23] V. Cavallo, A. Roggero, A. Fina, J. F. Gerard, and S. Pruvost, “P(MMA-co-MAA)/cellulose nanofibers composites: Effect of hydrogen bonds on molecular mobility,” *Carbohydr Polym*, vol. 346, p. 122579, Dec. 2024, doi: 10.1016/J.CARBPOL.2024.122579.
[24] J. Lara and H. P. Schreiber, “Specific interactions and adsorption of film-forming polymers,” *Journal of Coatings Technology*, vol. 63, no. 801, pp. 81–90, Oct. 1991, Accessed: May 13, 2025. [Online]. Available: https://www.scopus.com/record/display.uri?eid=2-s2.0-0026237165&origin=inward
[25] D. Y. Kwok, A. Leung, C. N. C. Lam, A. Li, R. Wu, and A. W. Neumann, “Low-Rate Dynamic Contact Angles on Poly(methyl methacrylate) and the Determination of Solid Surface Tensions,” *J Colloid Interface Sci*, vol. 206, no. 1, pp. 44–51, Oct. 1998, doi: 10.1006/JCIS.1998.5610.